

REPORT DOCUMENTATION PAGE

Form Approved
OMB No. 0704-0188

Public reporting burden for this collection of information is estimated to average 1 hour per response, including the time for reviewing instructions, searching existing data sources, gathering and maintaining the data needed, and completing and reviewing this collection of information. Send comments regarding this burden estimate or any other aspect of this collection of information, including suggestions for reducing this burden to Department of Defense, Washington Headquarters Services, Directorate for Information Operations and Reports (0704-0188), 1215 Jefferson Davis Highway, Suite 1204, Arlington, VA 22202-4302. Respondents should be aware that notwithstanding any other provision of law, no person shall be subject to any penalty for failing to comply with a collection of information if it does not display a currently valid OMB control number. PLEASE DO NOT RETURN YOUR FORM TO THE ABOVE ADDRESS.

1. REPORT DATE (DD-MM-YYYY) 17-06-2008		2. REPORT TYPE Technical Paper		3. DATES COVERED (From - To)	
4. TITLE AND SUBTITLE A Fast Method of Fully Characterizing Sputtering Angular Dependence (Preprint)				5a. CONTRACT NUMBER	
				5b. GRANT NUMBER	
				5c. PROGRAM ELEMENT NUMBER	
6. AUTHOR(S) Michael W. Gorrilla (AFRL/RZSA); Lubos Brieda & Michael Nakles (ERC)				5d. PROJECT NUMBER	
				5e. TASK NUMBER	
				5f. WORK UNIT NUMBER 33SP0853	
7. PERFORMING ORGANIZATION NAME(S) AND ADDRESS(ES) Air Force Research Laboratory (AFMC) AFRL/RZSS 1 Ara Drive Edwards AFB CA 93524-7013				8. PERFORMING ORGANIZATION REPORT NUMBER AFRL-RZ-ED-TP-2008-240	
9. SPONSORING / MONITORING AGENCY NAME(S) AND ADDRESS(ES) Air Force Research Laboratory (AFMC) AFRL/RZS 5 Pollux Drive Edwards AFB CA 93524-7048				10. SPONSOR/MONITOR'S ACRONYM(S)	
				11. SPONSOR/MONITOR'S NUMBER(S) AFRL-RZ-ED-TP-2008-240	
12. DISTRIBUTION / AVAILABILITY STATEMENT Approved for public release; distribution unlimited (PA #08238A).					
13. SUPPLEMENTARY NOTES For presentation at the 44 th AIAA Joint Propulsion Conference, Hartford, CT, 20-23 July 2008.					
14. ABSTRACT A new method has been demonstrated in which a single experiment is used to fully define the sputtering angular dependence of a given material. The method subjects a circular rod of test material to a mono-energetic and highly collimated ion beam. The eroded profile is then measured using optical profilometry; the full sputtering angular dependence curve is then extracted using a numerical approach.					
15. SUBJECT TERMS					
16. SECURITY CLASSIFICATION OF: a. REPORT Unclassified			17. LIMITATION OF ABSTRACT SAR	18. NUMBER OF PAGES 10	19a. NAME OF RESPONSIBLE PERSON Dr. Justin Koo
b. ABSTRACT Unclassified			19b. TELEPHONE NUMBER (include area code) N/A		
c. THIS PAGE Unclassified					

A fast method of fully characterizing sputtering angular dependence (PREPRINT)

Michael W. Gorrilla*, Lubos Brieda,† and Michael Nakles,‡

Air Force Research Laboratory, Edwards AFB, CA 93524, U.S.A.

and

Alexander C. Barrie§

Millennium Engineering and Integration, Greenbelt, MD 20708, U.S.A.

A new method has been demonstrated in which a single experiment is used to fully define the sputtering angular dependence of a given material. The method subjects a circular rod of test material to a mono-energetic and highly collimated ion beam. The eroded profile is then measured using optical profilometry; the full sputtering angular dependence curve is then extracted using a numerical approach.

I. Introduction

Understanding the sputtering characteristics of electric propulsion thruster materials is important for predicting lifetime and performance. Sputtered material is also a contamination concern as it can be redeposited and degrade system performance.

The amount of sputtered material is a function of the energy (velocity) and angle of incidence of the impacting ions. Although analytical sputtering profiles exist for some monatomic metals,¹ the sputtering behavior of materials used in EP applications is typically obtained experimentally using weight loss and quartz crystal microbalance (QCM) measurements.² In each case, a flat plate is eroded by an ion source at a certain energy and a certain angle of incidence. These traditional methods are characterized by the time consuming task of performing the multiple experimental runs necessary to achieve sufficient angular resolution.

The method presented in this paper was previously employed by Barrie³ et al. to measure the sputtering rate of an aluminum rod subjected to bombardment by Xenon particles from a 10 cm Hall Effect Thruster (HET). In this paper we investigate the effect of the non-uniform beam on the erosion profile by eroding three identical rods located at various axial distances from the thruster as well as differing angles from the thrust axis as seen in Figure 1 and Figure 2. The increased distance from the thruster results in a more uniform flow profile at the expense of a lower erosion rate.

II. Model

Yamamura gives the angular sputter yield as a correction factor to the normal sputter yield with Equation 1 below. The normal sputter yield, $Y(0)$, is calculated by Yamamura's method as summarized by Cheng.⁴ f and Σ are fit parameters tabulated for a limited number of source and target combinations in literature.¹ θ is the incident angle relative to the surface normal.

*Research Engineer, AFRL/RZSS, Member AIAA, michael.gorrilla@edwards.af.mil

†Research Engineer, ERC Inc., Member AIAA, lubos.brieda@edwards.af.mil

‡Research Engineer, AFRL/RZSS, Member AIAA, michael.nakles@edwards.af.mil

§Contamination Engineer, NASA/GSFC, Member AIAA, abarrie@gmail.com

$$\frac{Y(\theta)}{Y(0)} = \cos^{-f} \theta \exp -\Sigma(\cos^{-1} \theta - 1) \quad (1)$$

where,

$$f = f_s \left(1 + 2.5 \frac{1 - \zeta}{\zeta} \right), \quad (2)$$

$$\Sigma = f \cos \theta_{opt}, \quad (3)$$

$$\zeta = 1 - \sqrt{\frac{E_{th_ang}}{E}} \quad (4)$$

$$E_{th_ang} = 1.5 \frac{U_S}{\gamma} \left[1 + 1.38 \left(\frac{M_1}{M_2} \right)^h \right]^2 \quad (5)$$

$$h = 0.834, M_2 > M_1$$

$$h = 0.180, M_2 < M_1$$

Where M_1 and M_2 are the source and target atomic masses respectively.

$$\gamma = \frac{4M_1 M_2}{(M_1 + M_2)^2} \quad (6)$$

$$\theta_{opt} = 90^\circ - 286(\psi)^{0.45} \quad (7)$$

$$\psi = \left(\frac{a}{R_0} \right)^{3/2} \left[\frac{Z_1 Z_2}{(Z_1^{2/3} + Z_2^{2/3})^{1/2}} \frac{1}{E} \right]^{1/2} \quad (8)$$

Table 1 lists the required constants needed to calculate f and Σ and the angular dependence curve for Xenon sputtering Al.

Table 1. Published constants for Xe sputtering Al

Parameter	Al
M_1 amu	131.29
M_2 amu	26.982
Z_1 , source atomic number	54
Z_2 , target atomic number	13
f_s	1.8
a , screening radius	0.1052
R_0 , average lattice constant	2.56
U_S , sublimation energy [eV]	3.39

Using the parameters above and Equations 2-8 above one arrives at an f and Σ of 7.84 and 4.01 respectively using the expected incident energy of 220 eV. Equation 1 is plotted in Figure 5 with these values and a normal sputtering yield of unity.

Since the angular sputter yield depends on angle of incidence and incoming energy, a circular cylinder was placed in a uniform and mono-energetic flow. When a circular cylinder is subjected to a uniform flow perpendicular to its axis, the angles of incidence from 90° to 0° are achieved simultaneously. One would expect the greatest initial erosion to occur at the angle of optimal erosion, θ_{opt} , which is in the vicinity of 60° off the surface normal. Furthermore, the Yamamura model predicts no erosion when the flow is tangent to the surface ($\theta = 90^\circ$) and simply normal erosion when the flow is perpendicular to the surface ($\theta = 0^\circ$). Since we cannot measure erosion after a very short time, the surface is eroded over a long period of time resulting in the surface normals changing significantly. A numerical scheme was implemented to simulate the changing surface normals and allowed for the proper determination of f and Σ .

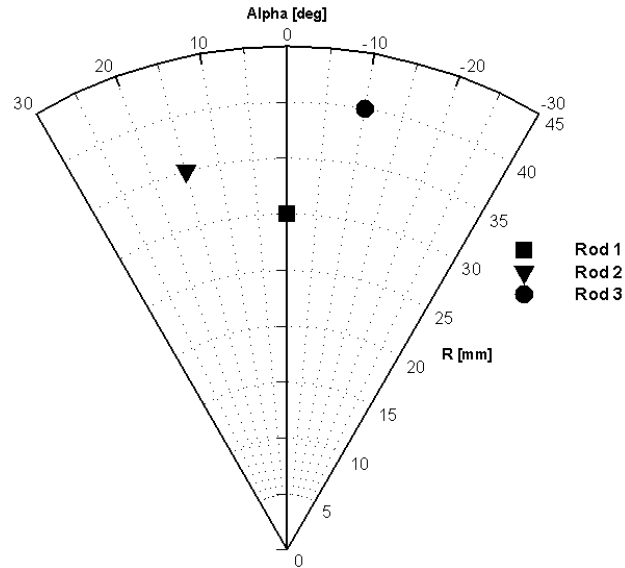


Figure 1. Placement of the rods in the chamber relative to the thruster, firing from $R = 0$ through $\alpha = 0^\circ$ parallel to the page.

III. Results

In an effort to subject the rods to a more uniform and mono-energetic flow of Xenon ions, the rods were placed at a greater distance from the source compared to the previous experiment and at various angles from the thrust axis. Locations beyond 15 degrees off the thrust axis and 30 cm from the source, plasma densities drop off quickly resulting in lower erosion rates. Figure 1 shows the rod positions relative to the thruster.

After firing for 135 hours the rods were removed from the vacuum chamber, exposed to the atmosphere and their surface profiles were measured using an optical profilometer. Ten circumferential scans were performed on each rod across a 1 mm swath centered at the height of the thruster. Each of the ten scans was averaged for each rod and this data was numerically smoothed to 128 points. Figure 3 shows the 64 smoothed points from each rod that experienced erosion. The uneroded profile is plotted in the same figure and has a radius of 3.98 mm. Rod 1 obviously eroded the most because it was the closest and was placed on the thrust axis whereas rods 2 and 3 eroded significantly less but in a similar way due to similar plasma densities.

The depth of erosion was calculated and plotted in Figure 4 and wings of higher erosion are apparent as sputter rates are higher at incident angles beyond normal. According to published fit parameters and Yamamura's model, initial erosion depth should be the highest around 60° , this was not observed because the surface was eroded to a measureable depth and consequently, the surface normals changed significantly. As the surface normals changed, the assumption of a uniform flow striking a circular cylinder is not valid and the surface erodes in a complex way.

The fit parameters were extracted from the eroded profiles in Figure 3 using a numerical simulation which applied Equation 1 on a meshed 2D circular model of the uneroded rod. In each simulation, the rod was eroded in very small steps according to Yamamura's model until the point of normal sputter yield $\theta = 0^\circ$ reached the respective measured normal sputter depth. This effectively normalizes the simulations in time and erosion rates need not be considered. An optimization routine was used to determine f and Σ values which yielded best agreement with the measured eroded profiles and are found in Table 2.

The sputter yield angular dependence curve is plotted in Figure 5 for each rod using the experimental fit parameters along with published results; the plots were normalized using a normal sputter yield of unity. It is immediately apparent the experimental curves predict lower sputter yields than the published curve. This could be due to the fact that the ion flow was not truly mono-energetic nor uniform as was assumed in the experiment. The angular dependence was not captured with rod 1 due to cross-flow from the thruster exit resulted in a wide range of normal incidence upon the rod. Rods 2 and 3 captured more of the angular dependence due to more ideal flow characteristics at their locations in plume. Rods 2 and 3 over

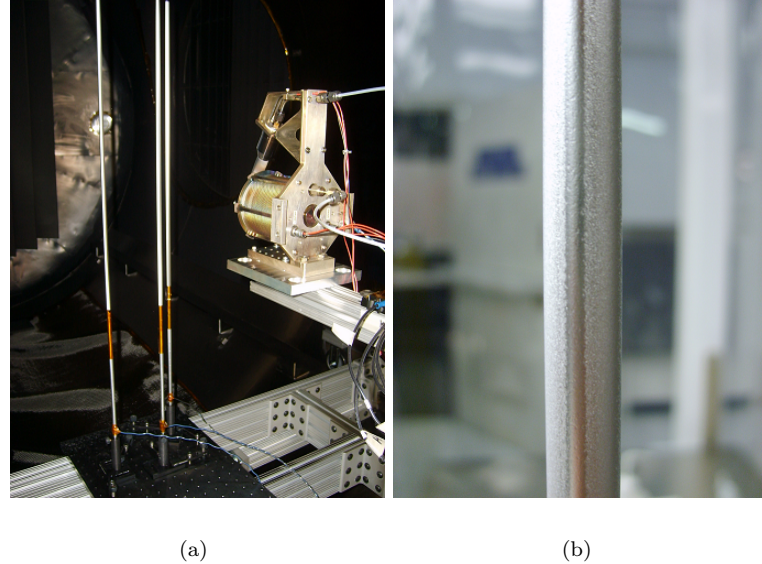


Figure 2. Experimental setup and clearly visible erosion

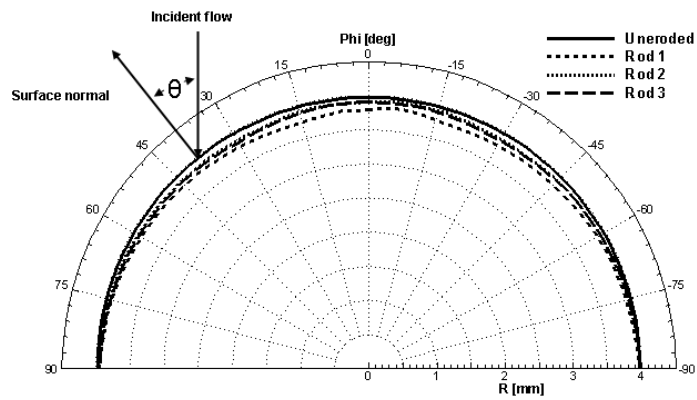


Figure 3. Eroded profiles of the three rods compared to the original rod.

and under predict the angle of optimal erosion respectively, this could be due to slight thruster misalignment as each rod was on either side of the thrust axis. Figure 6 compares the measured eroded profiles with the expected profile calculated numerically using published fit parameters, with Φ indicating the angular position along the rod. In each case, the simulation showed a characteristic maximum erosion yield at an angle of incidence of nearly 60° as expected. Experimental results show good agreement for shallow angles of incidence. As the angle of incidence increases; however, the expected erosion yield was not observed.

Figure 7 compares measured eroded profiles with their respective simulations using values of f and Σ from the optimizer routine. Figure 8 compares the simulated eroded profiles for each rod using their respective experimental values of f and Σ with that of the published published values. In each case, the surface mesh was eroded until the normal sputter yield matched with experimental measurements.

IV. Conclusion and Future Work

This work was a continuation of the experiment by Barrie³ in which a new method of determining the sputtering angular dependence characteristics of a material was studied. Current methods of determining the sputtering characteristics of a material involve multiple time consuming steps. This paper further studies the feasibility of determining the sputter yield angular dependence in a single measurement.

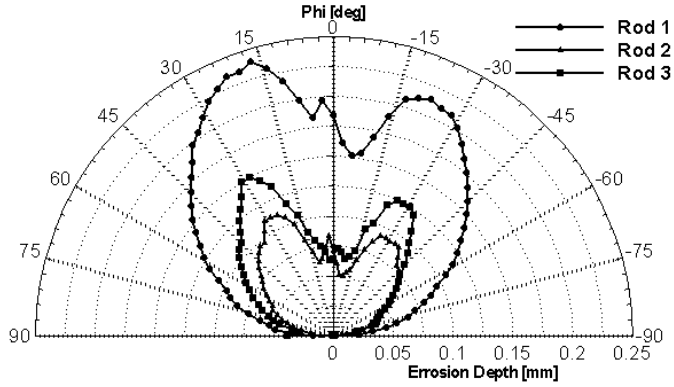


Figure 4. Erosion depth for the three rods as a function of angular position.

Table 2. Extracted f and Σ for the three rods and published values

	f	Σ
Rod 1	0.8	0.3
Rod 2	2.1	0.9
Rod 3	8.9	5.7
Published	7.84	4.01

Three ground aluminum circular cylinders were subjected to the plume of a HET thruster at differing off thrust axis angles and distances from the plume source. The cylinders were bombarded for 135 hours and visible erosion occurred. The eroded surfaces were measured using an optical profilometer and compared to their respective uneroded surfaces. Optimal fit parameters f and Σ for use in Yamamura's sputter yield angular dependence equation were then extracted from the measured profiles using an erosion simulator and an optimization routine. The extracted fit parameters yielded close agreement with experimental measurements.

The fit parameters calculated in this experiment did not match closely with published values, but were in better agreement than in the first attempt. Much of the sputter yield angular dependence was captured but not to the correct scale. By moving the rods farther away from the thruster exit and at greater angles away from the thrust axis, a more uniform and mono-energetic flow was achieved. The more uniform flow in this experiment subjected the rods to a flow closer to that which was assumed. The most likely reason for the discrepancy among the fit parameters is the nature of the HET plume structure. Even at the distances the rods were placed, cross-flow from the thruster exit introduced a certain degree of flow non-uniformity which altered way the rods were eroded.

A significant increase in accuracy of the experimental fit parameters compared to past work was achieved simply by moving the rods to a more uniform region of the HET plume; one would expect better results if a rod were placed even further. When using a HET for this experiment, a compromise exists between flow uniformity and the required time to erode to a measurable depth. A better source could be used such as an ion thruster which would yield the desired flow characteristics this experiment requires.

V. Acknowledgements

The authors would like to thank Dr. William Hargus for formulating the idea of sputtering a circular cylinder as means of measuring a material's erosion characteristics. Additional thanks goes to Mr. Bryan Taylor for his aid with the erosion and optimization routines employed in this work.

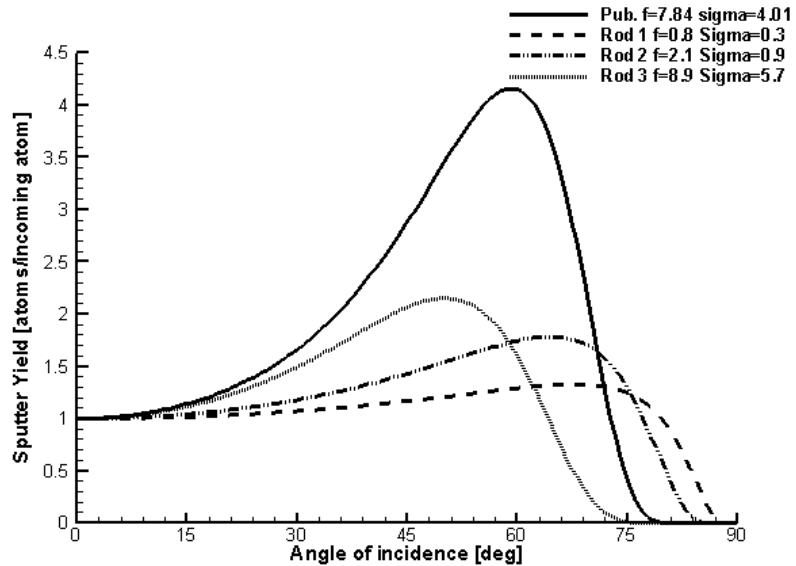


Figure 5. Sputtering yield as a function of incident angle.

References

¹Yamamura, Y., Y. Itikawa, and N. Itoh. IPPJ-AM-26, "Angular Dependence of Sputtering Yields on Monatomic Solids." Institute of Plasma Physics, Nagoya University, June 1983.

²Yalin, A. P., Williams, J. D., Surla, V., and Zoerb, K. A., "Differential Sputter Yield Profiles of Molybdenum due to Bombardment by Low Energy Xenon Ions at Normal and Oblique Incidence," Submitted to: *Journal of Physics D: Applied Physics*

³Barrie, A., Taylor, B., Ekholm, J., and Hargus, W., "Calculating Sputter Rate Angular Dependence Using Optical Profilometry," *30th International Electric Propulsion Conference*, IEPC-2007-001

⁴Cheng, S., *Computational Modeling of a Hall Thruster Plasma Plume in a Vacuum Tank*, Masters Thesis, Department of Aeronautics and Astronautics, Massachusetts Institute of Technology, 2002.

⁵Yamamura, Y. and Tawara, H., "Energy Dependence of Ion Induced Sputtering Yields From Monatomic Solids at Normal Incidence," *Atomic Data and Nuclear Tables*, Vol. 62, 1996.

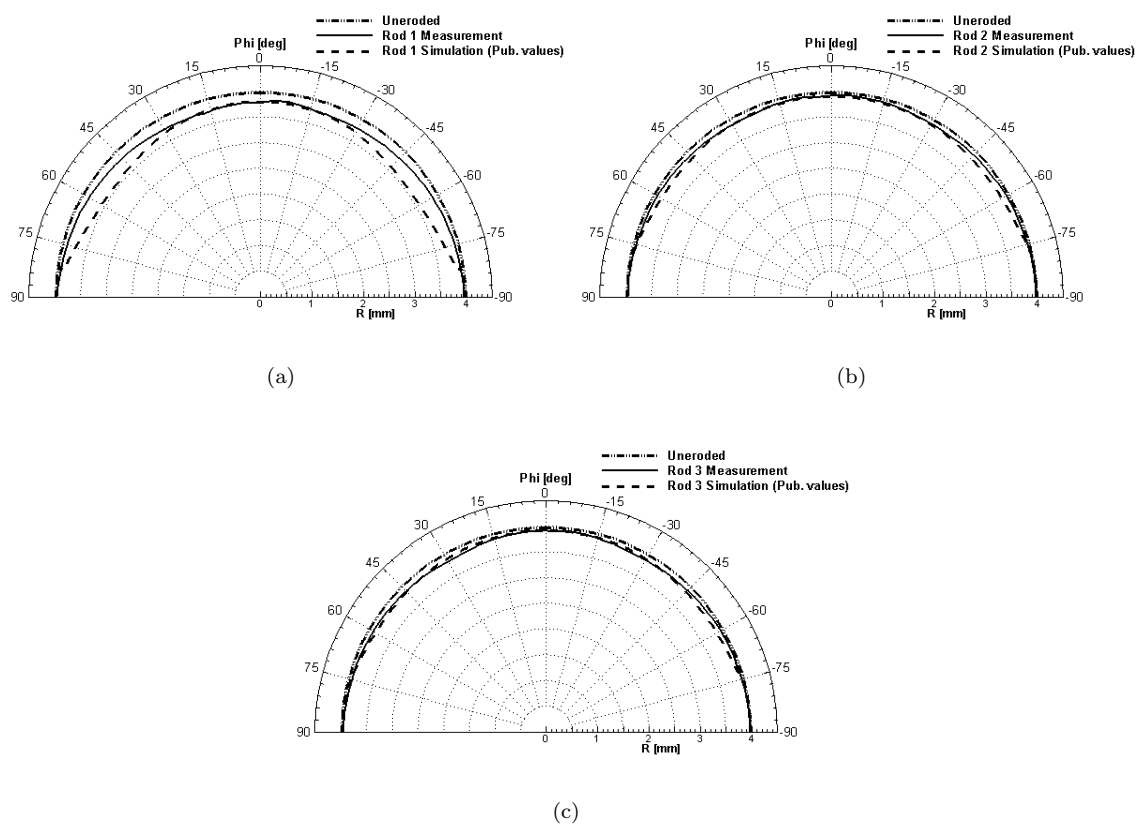


Figure 6. Comparison between measured rod profiles and simulations using published fit parameter values

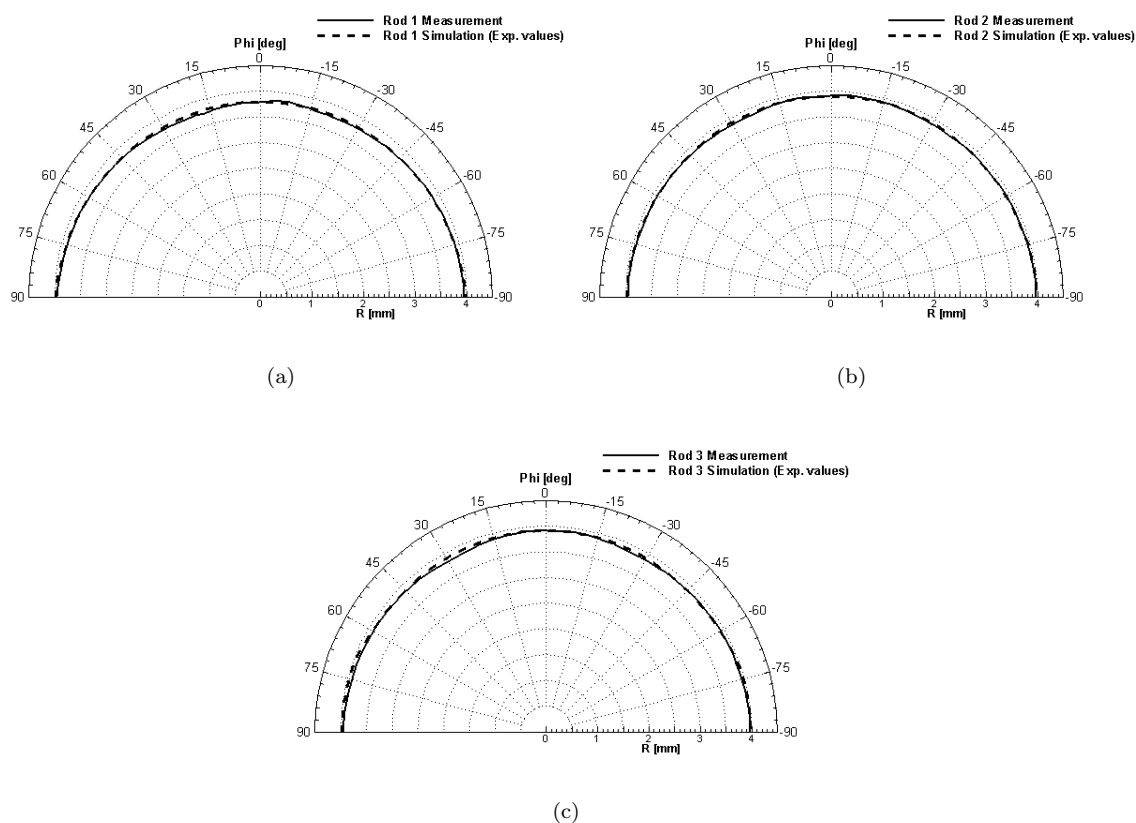


Figure 7. Comparison between measured rod profiles and simulations using extracted f and Σ values

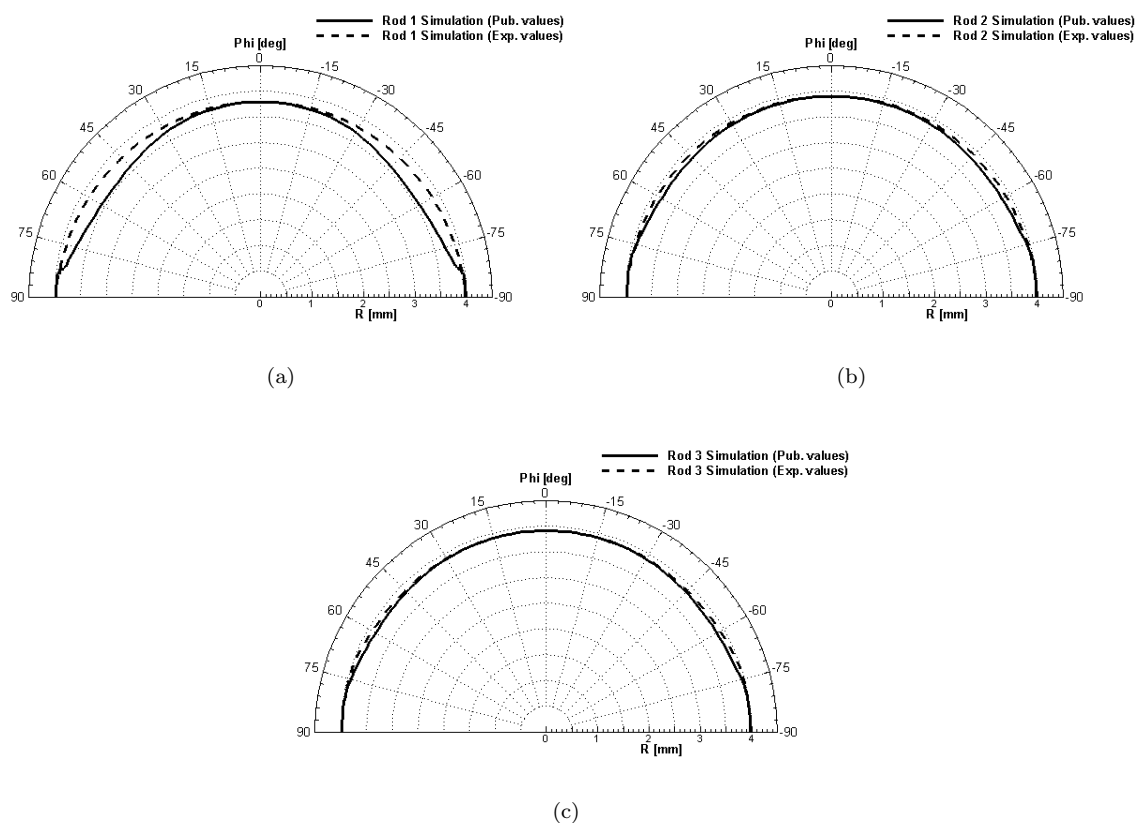


Figure 8. Comparison between simulations using published and extracted f and Σ values